

SPECTRAL EVOLUTION OF THE MICROQUASAR XTE J1550–564 OVER ITS ENTIRE 2000  
OUTBURSTJ. RODRIGUEZ<sup>1,2</sup>, S. CORBEL<sup>1,3</sup> AND J.A. TOMSICK<sup>4</sup>  
*accepted for publication in ApJ*

## ABSTRACT

We report on RXTE observations of the microquasar XTE J1550–564 during a  $\sim 70$  day outburst in April–June 2000. We present the PCA+HEXTE 3–200 keV energy spectra of the source, and study their evolution over the outburst. The spectra indicate that the source transitioned from an initial Low Hard State (LS), to an Intermediate State (IS) characterized by a  $\sim 1$  Crab maximum in the 1.5–12 keV band, and then back to the LS. The source shows an hysteresis effect such that the second transition occurs at a 2–200 keV flux that is half of the flux at the first transition. This behavior is similar to what observed in other sources and favors a common origin for the state transitions in soft X-ray transients. In addition, the first transition occurs at a  $\sim$  constant 2–200 keV flux, which probably indicates a change in the relative importance of the emitting media, whereas the second transition occurs during a time when the flux gradually decreases, which probably indicates that it is driven by a drop in the mass accretion rate. In both LS, the spectra are characterized by the presence of a strong power-law tail (Compton corona) with a variable high energy cut-off. During the IS, the spectra show the presence of a  $\sim 0.8$  keV thermal component which we attribute to an optically thick accretion disk. The inner disk radius as inferred from disk-blackbody fits to the energy spectrum remains relatively constant throughout the IS. This suggests that the disk may be close to its last stable orbit during this period. We discuss the apparently independent evolution of the two media, and show that right after the X-ray maximum on MJD 51662, the decrease of the source luminosity is due to a decrease of the power-law luminosity, at a constant disk luminosity. The detection of radio emission, with a spectrum typical of optically thin synchrotron emission, soon after the X-ray peak, and the sudden decrease of the power law luminosity at the same time may suggest that the corona is ejected and further detected as a discrete radio ejection.

*Subject headings:* accretion – black hole physics – stars: individual (XTE J1550–564)

## 1. INTRODUCTION

Soft X-ray transients (SXT) are accretion powered binary systems, hosting a compact object (either a neutron star or a black hole), which spend most of their life in quiescence, and are detected in X-rays as they undergo episodes of outburst. Their X-ray spectra are usually dominated by two components, representing different physical processes acting in the close vicinity of the accreting object. The soft X-rays are likely the spectral signature of an optically thick geometrically thin accretion disk, whereas the hard X-rays are interpreted as the inverse Compton scattering of the soft photons from the accretion disk on hot electrons present in an optically thin coronal medium. Depending on whether the electrons have a thermal velocity distribution or not, this “hard tail” can be characterized by the presence or absence of an exponential cut-off, at a given threshold energy. Based on the shape and strength of the spectra one can distinguish between 5 common spectral states thought to be linked to the accretion rate of the source (see *e.g.* Belloni 2001 for a recent review).

- The *Quiescent State* (hereafter QS), is the “off” state in which SXTs spend most of their lives. The observations of SXTs in such a state have shown

that the spectrum was power law like, with a photon index that could be either soft or hard (e.g. Kong et al. 2002). The luminosity is several orders of magnitude below that of the other states. The accretion disk is undetectable in the X-rays.

- In the *Low Hard State* (hereafter LS), the  $\nu - f_\nu$  spectrum is peaked in the hard X-rays, and characterized by a strong power law with a photon index  $\Gamma \sim 1.5 - 1.9$ , and a cut-off around 100 keV. The disk emission remains weak, and its innermost part has a temperature  $kT \leq 0.5$  keV.
- During the *Intermediate State* (hereafter IS) the contribution of the two spectral components to the overall luminosity is of the same order. The disk reaches a temperature of  $\sim 1$  keV, and the hard tail has a photon index of  $\Gamma \sim 2.5$ .
- In the *High Soft State* (hereafter HS) the soft ( $\leq 10$  keV) luminosity is high and the spectrum is dominated by a thermal component in that range. The temperature of the disk is  $\sim 1 - 1.5$  keV. The power law is faint with a steep photon index  $\Gamma \geq 2.5$ .

<sup>1</sup> DSM/DAPNIA/Service d’Astrophysique (CNRS URA 2052), CEA Saclay, 91191 Gif-sur-Yvette, France

<sup>2</sup> Integral Science Data Center, Chemin d’Ecogia, 16, CH-1290 Versoix, Switzerland

<sup>3</sup> Université Paris VII Fdration APC, 2 place Jussieu, 75005 Paris, France.

<sup>4</sup> Center for Astrophysics and Space Sciences, Code 0424, University of California at San Diego, La Jolla, CA 92093, USA

- In the *Very High State*, (hereafter VHS) the overall luminosity is close to the Eddington luminosity. The disk has a temperature  $kT \sim 1 - 2$  keV, and the power law is steep with  $\Gamma \sim 2.5$ , although both components contribute significantly to the luminosity. It should be noted that the VHS is spectrally intermediate between the LS and the HS (Rutledge et al. 1999), making then the IS and VHS similar states observed at different luminosities (Homan et al. 2001, see also Mndez & van der Klis, 1997).

A summary of the source history can be found in Rodríguez et al. (2003, hereafter paper 1). XTE J1550–564 is a microquasar (Hannikainen et al 2001, Corbel et al. 2002) hosting a black hole of  $10.5 \pm 1.5 M_{\odot}$  (Orosz et al. 2002), lying at a distance of  $3.2 \text{ kpc} \leq D \leq 10.8 \text{ kpc}$ , with a preferred distance of  $5.3 - 5.9 \text{ kpc}$  (Orosz et al. 2002). Extensive spectral and timing analysis of its 1998-1999 outburst has shown the need of an additional parameter beside the accretion rate  $\dot{M}$  to account for the X-ray state transitions (Homan et al. 2001).

Renewed X-ray activity of XTE J1550–564 was reported by Smith et al. (2000). The source underwent a  $\sim 70$  day outburst starting on 2000 April 6 (paper 1, and reference therein). Corbel et al. (2001) report the detection of a radio emission with a negative spectral index on MJD 51665. They attribute it to optically thin synchrotron emission from a discrete ejection. The date of the ejection event is however hard to constrain, and may correspond to the state transition occurring a few days before (Corbel et al. 2001). These authors also point out the absence of radio emission on MJD 51670, indicating that no jet feature is present during that time, and they detect radio emission with an inverted spectrum on MJD 51697, which they attribute to a compact jet. The outburst initiates in the IR and optical (Jain et al. 2001)  $\sim 10$  days before the X-rays, and a second IR/Optical maximum occurs as the source has returned to the LS around MJD 51690. This second IR-Optical peak is possibly related to the compact jet synchrotron tail (Corbel et al. 2001) as its inverted spectrum can extend up to the near IR range (Corbel & Fender, 2002). Tomsick, Corbel & Kaaret (2001) (hereafter TCK01) report spectral (RXTE+Chandra) observations during the very last part of the outburst, as XTE J1550–564 is returning to quiescence.

We have studied the behavior of a low frequency QPO in paper 1, and we focus here on the X-ray spectral behavior of XTE J1550–564 from the very beginning of the PCA+HEXTE pointed observations on MJD 51644, until MJD 51698 where the observations are contaminated both by the Galactic ridge diffuse emission and the close outbursting transient pulsar XTE J1543 – 568 (TCK01). We perform an analysis similar to that reported in TCK01 (covering MJD 51680–51698), and add the whole RXTE data set publicly available in the archives covering this outburst. We thus present for the first time the entire PCA+HEXTE spectral analysis of XTE J1550–564 over its 2000 outburst. The organization of the paper is as follows; we start by presenting the data reduction and analysis method used, before presenting the spectral evolution of the source. We discuss our results in the last part of the paper.

## 2. OBSERVATIONS

### 2.1. Data Reduction

XTE J1550–564 has been observed continuously with RXTE all over its outburst, *i.e.* from MJD 51644 (Apr. 10), to MJD 51741 (July 16). Since the background in the Galactic ridge is difficult to estimate with a non-imaging instrument, we restrict our study to the interval between MJD 51644 and MJD 51698, and refer the reader to the study of TCK01 for the following period.

We have reduced and analyzed the data using *LHEA-SOFT* package v5.2, which includes new response matrices and new background files for the PCA. We use here the maximum number of PCUs turned on over an observation, and both clusters of HEXTE. We restricted ourselves to the time when the elevation angle was above  $10^{\circ}$ , the offset pointing less than  $0.02^{\circ}$ , and we also rejected the data taken while crossing the SAA. In addition, the good time intervals (GTIs) were defined when the number of Proportional Counter Units (hereafter PCU) turned on was constant and equal to the maximum available over a given observation, for most of them, at least 3 PCUs were turned on. May 12, 2000 corresponds to the abrupt loss of Xenon layer in PCU 0, which renders its use for spectral analysis difficult and uncertain. We therefore extracted all the spectra from the top layer of all available PCUs, except PCU 0. All spectra from individual PCUs were summed during the extraction. Background spectra were estimated using *PCABCAKEST V.3.0*. The responses were generated with *pcarsp V8.0*.

HEXTE spectra were extracted from both clusters, in the standard mode data. We followed the “cook book” procedures for separating the ON and OFF positions before extracting the raw spectra (source and background), and then correct them for dead-time. Responses were estimated with *hxrsp V3.1*. The PCA+HEXTE resultant spectra of a single observation were then analyzed together in *XSPEC v11.1.0*. We retain in our fits the energy channels between 3 and 30 keV for the PCA, and between 18 and 200 keV for the HEXTE. Furthermore, in order to accommodate for uncertainties in the PCA response matrix, we included 0.8% systematic errors from 3–8 keV, and 0.4% from 8–30 keV (see TCK01).

### 2.2. Spectral analysis

Several models were tested in the course of the spectral analysis. In every fit, a multiplicative constant, representing the normalization between the instruments, was added to the spectral model in order to take into account the uncertainties in the PCA-HEXTE cross calibration. To determine the spectral models, we first fitted PCA+HEXTE from MJD 51646 and MJD 51648 with a simple model consisting of interstellar absorption (*wabs* in XSPEC terminology) plus a power law. The resultant  $\chi^2$  is poor (1191 for 142 dof), with large residuals around 6.5 keV and a broad minimum around 10 keV. As the RXTE bandpass is not ideally suited for the determination of the interstellar absorption, we applied the equivalent Hydrogen column density value  $N_H$  returned from recent CHANDRA observations (Kaaret et al. 2003), *i.e.*  $N_H = 0.9 \times 10^{22} \text{ cm}^{-2}$ , and froze it in all our fits.

Adding iron edge absorption (*smedge*) improves the fits significantly with  $\chi^2 = 942$  (139 dof). Following Sobczak et al. (1999), and TCK01, we froze the width of the *smedge* model to 10 keV. In order to accommodate for the high energy behavior (HEXTE band) an exponential cut-off at higher energy is needed and gives satisfactory fits with  $\chi^2 = 137$  (138 dof) for MJD 51646, and 144 (138 dof) for MJD 51648. Adding a Gaussian emission line around 6.5 keV gives only a marginal improvement to our fits. We also tentatively included a multi-color disk blackbody (Mitsuda et al. 1984), thought to represent the emission coming from the optically thick accretion disk, but our fits failed to achieve convergence, at least from MJD 51644 through MJD 51655. The spectral parameters returned from the fits are shown for the entire outburst in Table 1, and the spectrum of MJD 51644 is represented in the left panel of Fig. 1.

From MJD 51658 a soft excess is detectable in the spectra (Fig. 1 shows the example of MJD 51662). Using the model consisting of an absorbed (Hydrogen + Fe Edge) power law cut at high energy leads to poor  $\chi^2$  (153 for 138 dof, and even worse for the following days). The addition of a multi-color disk blackbody model (Mitsuda et al. 1984) to the fits greatly improves their quality ( $\chi^2 = 134$  for 136 dof on MJD 51658, although the disk radius parameter is difficult to constrain that day). Note that during IS/VHS, the multi-color disk model can give unreliable values of the inner radius (Sobczak et al. 1999, Merloni, Fabian & Ross 1999), especially when the ratio of the disk flux to the total flux is low (Merloni et al. 1999). The high energy cut-off is still needed until MJD 51662 (it is significant at the 99.5 % level using an F-test). We have checked its presence the following days by systematically adding an exponential cut off in our fits, but it gave no improvement to the fits (see Table 1). Over that period, the hard X-ray contribution has significantly decreased (Fig. 2), and the photon index ranges from  $\simeq 2.0$  to  $\simeq 2.4$ . The iron line may still be present but for the same reasons as explained above we did not include it in our analysis.

Around MJD 51683 the fits fail to converge if the blackbody component is kept in the model. From MJD 51682 until MJD 51688, an exponential cut-off is needed in the fits. We note, however, that for MJD 51686, 51687, and 51688, the resultant improvement in the fits becomes only marginal; we nonetheless kept this additional component. After MJD 51688 there is no convergence when the exponential cut-off is included in the model (see also TCK01). So that the last observations are fitted with a simple model consisting of interstellar and smeared edge ( $\geq 7$  keV) absorptions, and a power law.

Two of the observations were already reported by Miller et al. (2003, MJD 51667, 51670). Although they included a Gaussian feature in their fit, we note the relatively good agreement between their results and ours for both dates. The small differences can be due to the fact that they have used a value of  $0.8 \times 10^{22}$  cm $^{-2}$  for the  $N_H$  parameter, and have made joint Chandra+RXTE spectral fits.

The evolution of the spectral parameters are reported in Table 1 and they are plotted on Fig. 2. The source spectral behavior over the outburst can be divided into two distinct states as illustrated by Fig. 2. Based on the spectral parameters returned from the fits (Table 1), we identify, without any ambiguities, the initial rise as a standard LS (from MJD 51644 to MJD 51658). The evolution of the source is rather slow here; the photon index rises from  $1.49 \pm 0.01$  to  $1.70 \pm 0.01$  (Fig. 2), as the 2–60 keV flux slowly rises from  $1.3 \times 10^{-8}$  erg/cm $^2$ /s (MJD 51644) to  $2.0 \times 10^{-8}$  erg/cm $^2$ /s (MJD 51658). The exponential cut-off ranges from  $\sim 20$  to  $\sim 36$  keV, and presents no obvious correlation with the flux, whereas the folding energy decreases from  $\simeq 165$  keV, on MJD 51644 to  $\simeq 115$  keV on MJD 51658, with an increasing soft flux. MJD 51658 is still typical of a LS, with a photon index  $< 2$ , but here the spectrum has already started to soften (Fig. 2).

The state transition occurs on MJD 51660, where the hard tail steepens significantly with a photon index  $\geq 2$ . On MJD 51660 and 51662, however, a cut-off at high energy is still needed in the fits. We note that the folding energy increases up to  $\simeq 144$  keV on MJD 51660 and  $\simeq 422$  keV on MJD 51662. Based on the spectral parameters, we can identify this new state as an intermediate/very high state. It is difficult to distinguish between these two states since both have similar spectral and temporal behaviors (and may be the same state observed at different luminosities, Homan et al. 2001, Méndez & van der Klis 1997). The presence of high frequency QPOs (Miller et al. 2001) over the period of IS/VHS, does not help much in lifting the ambiguity. It is usually assumed that the VHS has a luminosity close to  $L_{Edd}$ , which in our case, assuming a  $10M_\odot$  black hole at 6 kpc (although the uncertainties are large), is  $\sim 1.3 \times 10^{39}$  erg/s. Here at the maximum (MJD 51662), the bolometric disk flux is  $2.1 \times 10^{-8}$  erg/cm $^2$ /s, and the 2–500 keV (extrapolated) power-law flux is  $3.35 \times 10^{-8}$  erg/cm $^2$ /s, giving a bolometric luminosity close to  $\sim 2.3 \times 10^{38}$  erg/s. Given the flux and in comparison with the previous outburst (Sobczak et al. 1999), we will refer to this state as an IS.

The spectral evolution from MJD 51660 to MJD 51662, is rather abrupt (Fig. 2), and suggests that the source has undergone dramatic evolution. Indeed, the power law tail is now much steeper, the disk temperature higher, and the folding energy of the cut-off has increased by a factor of  $\sim 3$ . The (color) radius obtained from the spectral fits (Fig. 2) varies between  $\simeq 32$  to  $\simeq 146$  km (assuming a distance of 6 kpc, for  $73.1^\circ$  inclination). Its value remains constant around 45–55 km over 13 observations. The disk reaches its highest temperature on MJD 51662, and from MJD 51665 until MJD 51674 its color temperature is around 0.75–0.8 keV and is found fairly constant (Fig. 2). After that, it starts to decrease down to  $\sim 0.5$  keV on MJD 51682. We note here that, although the color temperature decreases, the color radius seems to decrease also. This may be due to the difficulty in determining this parameter from spectral fits starting above 3 keV at times where the source count rate starts to be low (compared to e.g. MJD 51658, where although the disk has a lower color temperature, the counting statistics allow a better estimate of the parameters).

After MJD 51680, the source slowly returns into a LS

Date (MJD)	Photon Index	Color Radius* (km)	Disk Temp. (keV)	$E_{cut-off}$ (keV)	$E_{fold}$ (keV)	Red. $\chi^2$ (d.o.f.)
51644.4	1.49 ± 0.01			33.8 <sup>+2.0</sup> <sub>-2.1</sub>	165 ± 7	1.10 (138)
51646.3	1.46 ± 0.01			33.6 <sup>+2.8</sup> <sub>-3.0</sub>	137 <sup>+8</sup> <sub>-7</sub>	0.99 (138)
51646.6	1.48 ± 0.01			35.9 <sup>+2.3</sup> <sub>-2.5</sub>	127 <sup>+6</sup> <sub>-5</sub>	1.26 (138)
51648.7	1.47 ± 0.01			33.3 ± 1.6	123 <sup>+4</sup> <sub>-3</sub>	1.04 (138)
51650.7	1.47 ± 0.01			30.3 ± 1.8	120 ± 4	1.24 (138)
51651.4	1.48 ± 0.01			31.9 <sup>+1.7</sup> <sub>-1.5</sub>	122 <sup>+3</sup> <sub>-4</sub>	1.34 (138)
51652.2	1.47 ± 0.01			33.6 <sup>+1.6</sup> <sub>-2.0</sub>	111 ± 4	1.11 (138)
51653.5	1.50 ± 0.01			32.1 <sup>+1.2</sup> <sub>-1.3</sub>	109 ± 3	1.00 (138)
51654.7	1.51 ± 0.01			29.7 ± 1.5	109 ± 3	0.96 (138)
51655.7	1.55 ± 0.01			30.7 <sup>+1.7</sup> <sub>-2.1</sub>	111 ± 5	0.97 (138)
51658.6	1.70 ± 0.01	146 <sup>+1413</sup> <sub>-108</sub>	0.37 ± 0.014	19.4 <sup>+1.6</sup> <sub>-1.5</sub>	115 ± 5.6	0.98 (136)
51660.0	2.05 ± 0.02	47 <sup>+19</sup> <sub>-12</sub>	0.60 ± 0.06	18.7 <sup>+1.1</sup> <sub>-0.7</sub>	144 <sup>+8</sup> <sub>-7</sub>	0.92 (136)
51662.2	2.33 ± 0.02	32.5 <sup>+2.5</sup> <sub>-1.3</sub>	0.95 ± 0.04	17.7 <sup>+4.3</sup> <sub>-2.0</sub>	422 <sup>+216</sup> <sub>-80</sub>	0.86 (136)
51664.4	2.37 ± 0.02	45.6 <sup>+0.9</sup> <sub>-1.5</sub>	0.86 ± 0.01			1.05 (138)
51664.6	2.35 ± 0.02	42.4 ± 1.5	0.89 ± 0.01			1.43 (138)
51665.4	2.38 ± 0.02	52.0 <sup>+2.7</sup> <sub>-1.9</sub>	0.80 ± 0.01			1.00 (138)
51667.7	2.28 ± 0.02	47.8 <sup>+2.4</sup> <sub>-1.3</sub>	0.82 ± 0.02			0.95 (138)
51668.8	2.28 ± 0.02	47.8 <sup>+1.4</sup> <sub>-1.3</sub>	0.80 ± 0.01			1.07 (138)
51669.2	2.30 ± 0.01	49.5 <sup>+1.9</sup> <sub>-1.7</sub>	0.78 ± 0.01			1.18 (138)
51670.5	2.28 ± 0.01	53.0 <sup>+2.2</sup> <sub>-1.5</sub>	0.77 ± 0.02			1.02 (138)
51670.8	2.26 ± 0.02	49.7 <sup>+1.9</sup> <sub>-2.3</sub>	0.78 ± 0.01			0.87 (138)
51671.4	2.30 ± 0.02	50.8 <sup>+1.8</sup> <sub>-2.0</sub>	0.75 ± 0.01			1.06 (138)
51672.4	2.27 ± 0.02	55.2 ± 2.2	0.75 ± 0.02			1.08 (138)
51672.9	2.32 ± 0.01	51.0 <sup>+3.0</sup> <sub>-1.7</sub>	0.77 ± 0.02			1.20 (138)
51673.4	2.31 ± 0.01	39.4 <sup>+2.5</sup> <sub>-2.0</sub>	0.77 ± 0.02			1.28 (138)
51674.7	2.16 ± 0.02	45.0 ± 2.4	0.77 ± 0.02			1.52 (133)
51675.4	2.22 ± 0.01	43.8 ± 1.8	0.67 ± 0.02			0.92 (138)
51676.4	2.18 ± 0.01	46.1 <sup>+5.1</sup> <sub>-4.9</sub>	0.65 ± 0.03			1.16 (138)
51678.5	2.06 ± 0.01	46.5 <sup>+6.3</sup> <sub>-4.7</sub>	0.54 ± 0.05			1.23 (138)
51680.4	2.01 ± 0.01	53.5 <sup>+17.8</sup> <sub>-14.0</sub>	0.56 ± 0.06			1.16 (138)
51682.3	1.76 ± 0.01	39 <sup>+20</sup> <sub>-12</sub>	0.5 ± 0.1	30.3 <sup>+6.2</sup> <sub>-4.9</sub>	198 <sup>+37</sup> <sub>-32</sub>	0.93 (136)
51683.8	1.638 ± 0.005			60.5 <sup>+7.4</sup> <sub>-6.6</sub>	197 <sup>+38</sup> <sub>-31</sub>	0.84 (138)
51684.8	1.647 ± 0.007			59.2 <sup>+23.1</sup> <sub>-9.9</sub>	185 <sup>+63</sup> <sub>-55</sub>	0.91 (138)
51686.3	1.60 ± 0.01			76.4 <sup>+12.6</sup> <sub>-11.6</sub>	302 <sup>+257</sup> <sub>-108</sub>	1.00 (138)
51687.2	1.53 ± 0.01			55.8.4 <sup>+11.0</sup> <sub>-11.5</sub>	202 <sup>+78</sup> <sub>-52</sub>	1.17 (138)
51688.8	1.49 ± 0.01			31.8 <sup>+11.7</sup> <sub>-17.8</sub>	338 <sup>+114</sup> <sub>-65</sub>	0.78 (138)
51690.7	1.48 ± 0.02					1.05 (140)
51690.9	1.53 ± 0.01					1.32(140)
51692.5	1.48 ± 0.01					1.17 (140)
51693.4	1.50 ± 0.02					1.07 (140)
51695.2	1.50 ± 0.02					0.87 (140)
51696.4	1.53 ± 0.01					1.04 (140)
51698.9	1.59 ± 0.05					0.90 (140)

TABLE 1

BEST FIT PARAMETERS RETURNED FROM THE FITS OVER THE WHOLE OUTBURST.

$$*R_{col}/1km = \sqrt{\frac{Norm}{\cos i}} \times \frac{D}{6kpc}, \text{ WHERE } i = 73.1^\circ \text{ (SEE OROSZ ET AL. 2002).}$$

(see TCK01 for the spectral analysis of the observations after MJD 51680). Although the transition to the final low state is not as sharp as in the initial stage, there is a clear evolution in terms of spectral parameters, between MJD 51680 and MJD 51682, where the spectrum gets harder (Fig. 2), and manifests a cut-off at high energies (Table 1). From MJD 51682 to 51698 the source is in a LS, which first shows the presence of an exponential cut-off at high energy (MJD 51682-51688), while the following observations do not show any cut-off up to 200 keV.

Our timing analysis (paper 1) further confirms the nature of the states. During both states, we detect low frequency QPOs in the range 0.1–10 Hz. Two types of LFQPOs seem to be present over the outburst. The first type resembles the type C QPO (Remillard et al. 2002), and the other is more likely a type A. Interestingly, the presence of type C QPO is not related to the spectral state of the source, since it disappears after the X-ray peak on MJD 51662 (Fig. 2), well after the first transition, and reappears after the secondary peak, on MJD 51674, before the second transition. During the LS, however, it has a high amplitude (10–16 % RMS), and during the IS it is fainter (5%) as usually observed.

#### 4. DISCUSSION

##### 4.1. *Hard Component Evolution During the Initial Hard State*

Although recent studies have shown that the high energy emission could originate in a compact jet (Markoff, Falcke & Fender, 2001; Markoff et al. 2003), the results we present here will be discussed in the context of the standard Comptonization model involving a corona. We note, however that the coronal geometry is unclear, and the corona could be seen as the base of the jet.

In the standard Comptonization picture, the folding energy of the cut-off is close to the electron temperature. The slight decrease of the folding energy between MJD 51644–51658 may indicate that the Compton cloud is cooled more efficiently. This might correspond to the approach of the accretion disk (decreasing inner radius), while its inner temperature and the soft X-ray flux increase. This interpretation is in good agreement with the state transition observed on MJD 51660, and the presence of a thermal component in our fits from MJD 51658. This is also in good agreement with the observation of an infrared-optical luminosity peak with a spectrum that is compatible with a thermal emission, occurring 10 day before that in the X-ray (Jain et al. 2001). In that case, the 10 day delay between the infrared/optical and the X-rays would indicate that the accretion disk fills on a viscous time scale suggesting that it is truncated at a certain distance from the black hole.

The fact that the photon index evolves from  $\Gamma = 1.57$  on MJD 51655 to  $\Gamma = 1.74$  on MJD 51658 (Fig. 2) may indicate that the state transition initiates first by a change in the Compton medium. As already suggested from the analysis of the Unconventional Stellar Aspect (USA) data (Reilly et al. 2001) the situation could be similar to the two component accretion flow proposed in the case of other sources (Smith, Heindl & Swank, 2002). In that case, both flows possess their own response time-scale to any external perturbation (of the accretion rate). In a standard thin

disk it corresponds to the viscous time-scale  $t_{visc} \sim \frac{R^2}{\nu}$  ( $R$  being the radial distance to the black hole, and  $\nu$  the kinematic viscosity, usually parameterized with the  $\alpha$  prescription), which is then of the order of days (Frank, King & Raine, 1992). The coronal time-scale is the free fall time-scale, which is much shorter. In this picture, any external change in the accretion rate would first have an incidence on the corona, and then on the disk. We should note here that the evolution of XTE J1550–564 during this LS is very similar to that of the 1998 outburst (Wilson & Done, 2001; Wu et al. 2002). This suggests a common evolution for both outbursts although XTE J1550–564 did not reach the same X-ray luminosity during the 2000 outburst.

##### 4.2. *State Transitions and Hysteresis Effect Between the Two LS*

The first transition occurs at a total 2-200 keV flux of  $\sim 2.3 \times 10^{-8}$  erg/cm<sup>2</sup>/s on MJD 51660, and the second on MJD 51682 with a total 2-200 keV flux of  $1.1 \times 10^{-8}$  erg/cm<sup>2</sup>/s. The first transition is rather abrupt and occurs at a roughly constant flux, whereas the second is smoother and occurs while the source flux is monotonically decreasing, at a flux half that of the first one. We have plotted on Fig. 3 (left panel) the evolution of the spectral index vs. the 2–200 keV flux over the outburst. The figure shows an hysteresis, similar to what is observed in other black hole sources (Miyamoto et al. 1995, Nowak et al. 2002), and possibly in the neutron star Aql X–1 (Maccarone & Coppi 2003). In order to have a direct comparison with the latter source, we have plotted on Fig 3 (right panel) the ratio of the 2–50 keV powerlaw (corona) flux to the 2–50 keV disk-blackbody flux versus the 2–50 keV source flux. The behavior of XTE J1550–564 is here similar to that of Aql X–1 shown on Fig. 1 of Maccarone & Coppi (2003). In addition, Maccarone & Coppi (2003) have shown that the evolution of the hardness ratio versus the soft (1–12 keV) X-ray flux, i.e. the evolution of a given source in terms of spectral states versus source flux, was very similar for at least 4 black hole SXTs (XTE J1550–564, XTE J1859+326, XTE J2012+381, and probably XTE J1748–288, in addition to those previously reported by Miyamoto et al. 1995, i.e. GX 339–4, GS 1124–683 and Cyg X–1, and Nowak et al. 2002, GX 339–4), with the occurrence of a hysteresis loop. This similarity, both with black hole systems, and at least one neutron star system suggests that the state transitions, and the spectral evolution of those sources over their outbursts, obey similar mechanisms.

The fact that the first transition occurs at constant flux is not what is expected if we assume that the increase of the luminosity is due to an increase of the accretion rate alone. This behavior more likely reflects a change in the relative importance of the emitting media as pointed out by Zhang et al. (1997) in the case of Cyg X–1. This would further confirm the need of an additional parameter (beside the accretion rate) to model the state evolutions of LMXBs in outburst as already pointed out by Homan et al. (2001) during the previous outburst of XTE J1550–564, and Smith et al. (2002) for other sources. The additional parameter beside the accretion rate may then be related to the relative geometry disk-corona (e.g. the corona size as suggested by Homan et al. 2001). In that case a stable

accretion rate will produce the same amount of energy, and the relative geometry of the disk-corona system will modify the spectral energy distribution.

During the decline of the outburst, the transition towards the LS occurs while the flux is dropping similarly in all spectral bands (Fig. 2). This behavior is what expected if the state transition is driven only by variations of the accretion rate. In addition, when comparing the two different LS, one can see that the folding energy of the cut-off is systematically higher during the second LS (when present). This indicates that the coronal temperature is higher during the second LS. If we assume that the electron temperature depends on the flux of soft photons from the disk, the higher folding energy after the outburst may indicate that the disk recedes faster than it approaches the black hole. Although our observations seems to indicate rather constant physical parameters for the disk (Fig. 2), the fact that the disk is suddenly not detected soon after the transition, at times where the cut-off re-appear in the spectra, provides evidence for this possibility. The recession of the disk is compatible with the observation of a 65 Hz QPO by Kalemci et al. (2001), which seems to be of the same type as the HFQPO previously seen during the brightest part of the outburst (Miller et al. 2001).

#### 4.3. The Intermediate State: Accretion Disk Behavior

The presence of a cut-off in the spectra of MJD 51660 and MJD 51662 suggests that the coronal electrons have still a thermalized velocity distribution, although the photon index is soft. Those days also, the disk starts contributing significantly to the overall luminosity. So, in the standard picture of Comptonization, as the amount of cool thermal photons increases, the coronal electron temperature should decrease due to the higher cooling rate. The observation of an increasing folding energy for the cut-off between MJD 51658 and MJD 51662 argues, on the contrary, for coronal heating. This behavior is similar to what is observed by TCK01 although during the decay. They suggest that this might be the signature of the onset of different emission mechanism (e.g. bulk motion Comptonization).

According to Merloni et al. (1999), low values of the disk radius and flux ratio hide some failures in the basic multi-color disk-blackbody model. In a previous work (Rodríguez et al. 2002a), we have retained the radius values in our analysis only when  $\frac{F_{bbody}}{F_{tot}} > 0.5$ , with the fluxes estimated between 2–50 keV. This criterion is more stringent than that of Merloni et al. (1999), and has allowed us to study the disk radius behavior with high accuracy (Rodríguez et al. 2002a). On MJD 51662, the  $\sim 2-50$  keV disk unabsorbed flux is  $8.4 \times 10^{-9}$  erg/cm<sup>2</sup>/s, giving a  $\sim 25\%$  contribution to the total flux. It is very likely, then, that the disk parameters returned from the fit this day are unreliable. The disk behavior over the 2000 outburst resembles that of the 1998 outburst (at least during the first part of the latter reported in Sobczak et al. 1999). Although the peak temperatures, and the luminosities of the two outbursts differ significantly, there are, in both cases periods of relatively constant disk parameters. During these, the temperatures are in the same ranges (0.5–0.9 keV, Table 1 in Sobczak et al. 1999,

Table 1 in the current study). Given the constancy of the disk parameters, especially the inner radius over the IS (Fig. 2), and the similarity with the huge 1998-1999 outburst, it is tempting to consider that the disk is close to the last stable orbit. The presence, over this period, of high frequency QPOs (251 – 276 Hz, Miller et al. 2001), almost the highest values as yet observed in this source (285 Hz, Remillard et al. 1999, Homan et al. 2001), may further support this assumption (see also Kalemci et al. 2001).

#### 4.4. Ejection of the corona ?

Corbel et al. (2001) report the detection of radio emission with a flux density  $\propto \nu^{-0.46}$ . The negative spectral index is indicative of optically thin synchrotron emission, that Corbel et al. (2001) attribute to a discrete ejection of material from the system. This detection of a discrete ejection, which might be associated with the state transition (Corbel et al. 2001), raises the question of the origin of the ejected material. If the ejection is associated with the transition, this may indicate that the Comptonizing medium is the source of the ejection of the material as suggested in GRS 1915+105 (Rodríguez et al. 2002b). The ejection may also be triggered at the peak of luminosity, soon after MJD 51662. Indeed, if we plot the 2–50 keV unabsorbed black body flux vs. the 2–50 keV unabsorbed power-law flux (Fig. 4), it appears that after the 1 Crab flare (the extreme right point in Fig. 4), as the total luminosity is decreasing (Fig.2), the disk blackbody flux remains  $\sim$  constant during an initial period, while it is the power-law flux which decreases significantly. Given the relative constancy of the photon index those days (Fig. 2 and 3), this may suggest that there is less Compton scattering of the soft photons. A possible reason is that a part of the Compton medium is ejected. Given the detection of ejected material, it is tempting to consider that the Compton medium may be blown away, and not, as usually assumed, the innermost part of the disk.

Here again it is interesting to compare this outburst with the 1998-1999 one. During the latter outburst a discrete ejection of relativistic plasma (with apparent superluminal motion) was also detected right after the X-ray peak luminosity (Hannikainen et al. 2001). Both outbursts have very similar initial stages, starting with LS, reaching a peak in luminosity soon after a state transition, and a discrete ejection coincident with the spike in the 1998 outburst, and possibly coincident with the spike during the 2000 outburst. It is very interesting to note the similarities in the behavior of the source during both outbursts. In 1998 the huge X-ray spike is associated with large superluminal ejection (Hannikainen et al. 2001, Corbel et al. 2002), during the 2000 outburst the X-ray spike is associated with a discrete ejection of smaller amplitude. This may point out a strong coupling between the X-ray behavior and ejection of material in XTE J1550–564.

However the observation of Corbel et al. (2001) does not allow us to determine the date of ejection. Future multi-wavelength monitoring of SXTs in outburst, should allow to study better the accretion-ejection coupling as has been done for jet sources e.g. GRS 1915+105, GX 339–4. In the near future, this can be done also by including in multi-

wavelength studies the high energy broad band spectra from the soft X-rays with RXTE, up to the gamma rays with INTEGRAL.

J.R. would like to thank D. Barret, Ph. Durouchoux, J.-M. Hameury, G. Henry, E. Kalemci, M. Tagger, and P. Varnire for useful discussions. J.R. acknowledges financial

support from the French spatial agency (CNES). J.A.T. acknowledges partial support from NASA grant NAG5-13055. The authors thanks the anonymous referee for useful comments. This research has made use of data obtained through the High Energy Astrophysics Science Archive Center Online Service, provided by the NASA/Goddard Space Flight Center.

## REFERENCES

- Belloni T., 2001, proceedings of the JHU/LHEA workshop, “X-rays from Accretion onto Black Holes”, June 20-23 / astro-ph 0112217.
- Corbel S., Kaaret P., Jain R.K., Baylin C.D., Fender R.P., Tomsick J.A., Kalemci E., McIntyre V., Campbell-Wilson D., Miller J.M., McCollough M.L., 2001, *ApJ*, 554, 43.
- Corbel S., Fender R.P., Tzioumis A.K., Tomsick J.A., Orosz J.A., Miller J.M., Wijnands R., Kaaret P., 2002, *Science*, 298, 196.
- Corbel S. & Fender R.P., 2002, *ApJ*, 573, 35.
- Frank J., King A., Raine D., 1992, “Accretion Power in Astrophysics”, Cambridge Astrophysics Series.
- Hannikainen D., Campbell-Wilson D., Hunstead R., McIntyre V., Lovell J., Reynolds J., Tzioumis T., Wu K., 2001, *Ap& SS*, 276, 45.
- Homan J., Wijnands R., van der Klis M., Belloni T., van Paradijs J., Klein-Wolt M., Fender R.P., Méndez M., 2001, *ApJS*, 132, 377.
- Jain R.K., Baylin C.D., Orosz J.A., McClintock J.E., Remillard R.A., 2001, *ApJ*, 554, L181.
- Kaaret P., Corbel S., Tomsick J.A., Fender R., Miller J.M., Orosz J.A., Tzioumis T., Wijnands R., 2003, *ApJ*, 582, 945.
- Kong A.K.H., McClintock J.E., Garcia M.R., Murray S.S., Barret D., 2002, *ApJ*, 570, 277.
- Kalemci E., Tomsick, J. A., Rothschild R. E., Pottschmidt K., Kaaret P., 2001, *ApJ*, 563, 239, **K01**.
- Maccarone T.J., Coppi P.S., 2003, *MNRAS*, 338, 189.
- Markoff S., Falcke H., Fender, R., 2001, *A&A*, 372, L25.
- Markoff S., Nowak M.A., Corbel S., Fender R.P., Falcke H., 2003, *A&A*, 397, 645.
- Mndez M., van der Klis M., 1997, *ApJ*, 479, 926.
- Merloni A., Fabian A. C., and Ross R.R., 2000, *MNRAS*, 313, 193.
- Miller J.M., Wijnands R., Homan J., Belloni T., Pooley D., Corbel S., Kouveliotou C., van der Klis M., Lewin H.G., 2001, *ApJ*, 563, 928.
- Miller J.M., Marshall H.L., Wijnands R., DiMatteo T., et al., 2003, *MNRAS* 338, 7.
- Mitsuda K., Inoue H., Koyama K., Makishima K., Matsuoka M., Ogawara Y., Suzuki K., Tanaka Y., Shibazaki N., Hirano T., 1984, *PASJ*, 36, 741.
- Miyamoto, S., Kitamoto S., Hayashida K., Egoshi W., 1995, *ApJ*, 442, L13.
- Nowak M.A., Wilms J., Dove J.B., 2002, *MNRAS*, 332, 856.
- Orosz J.A., Groot P.J., van der Klis M., McClintock J.E., Garcia M.R., Zhao P., Jain R.K., Bailyn C.D., Remillard R.A., 2002, *ApJ*, 562, 568.
- Reilly K.T., Bloom E.D., Focke W., Giebels B., Godfrey G., Sz Parkinson P.M., Shabad G., Ray P.S., Bandyopadhyay R.M., Wood K.S., Wolff M.T., Fritz G.G., Hertz P., Kowalski M.P., Lovelette M.N., Yentis D.J., 2001, *ApJ*, 561, L183.
- Remillard R.A., McClintock J.E., Sobczak G.J., Bailyn C.D., Orosz J.A., Morgan E.H., Levine A.M., 1999, *ApJ*, 517, L130.
- Remillard R.A., Muno M.P., McClintock J.E., Orosz J.A., 2002, *ApJ*, 580, 1030.
- Rodriguez J., Varnière P., Tagger M., Durouchoux P., 2002a, *A&A*, 387, 487.
- Rodriguez J., Durouchoux P., Mirabel F., Ueda Y., Tagger M., Yamaoka K., 2002b, *A&A*, 386, 271.
- Rodriguez J., Corbel S., Kalemci E., Tomsick J.A., Tagger M., 2002, *submitted to ApJ*, paper 1.
- Rutledge R.E., Lewin W.H.G., van der Klis M., van Paradijs J., Dotani T., Vaughan B., Belloni T., Oosterbroek T., Kouveliotou C., 1999, *ApJS*, 124, 265.
- Smith D.A., 1998, *IAU Circ.* 7008.
- Smith D.A., Levine, A.M., Remillard R., Fox D., Schaefer R., RXTE/ASM Team, 2000, *IAU Circ.* 7394.
- Smith D.M., Heindl W.A., Swank J.H., 2002, *ApJ*, 569, 362.
- Sobczak G.J., McClintock J.E., Remillard R.A., Levine A.M., Morgan E.H., Baylin C.D., Orosz J.A., 1999, *ApJ*, 517, L121.
- Sobczak G.J., McClintock J.E., Remillard R.A., Cui W., Levine A.M., Morgan E.H., Orosz J.A., Baylin C.D., 2000, *ApJ*, 531, 537.
- Tomsick J.A., Corbel S., Kaaret P., 2001, *ApJ*, 563, 229.
- Wilson C.D., Done C., 2001, *MNRAS*, 325, 167.
- Wu K., Soria R., Campbell-Wilson D., Hannikainen D., Harmon B.A., Hunstead R., Johnston H., McCollough M., McIntyre V., 2002, *ApJ*, 565, 1161.
- Zhang S.N., Harmon B.A., Paciesas W.S., Remillard R.E., van Paradijs J., *ApJ*, 477, L95, 1997.

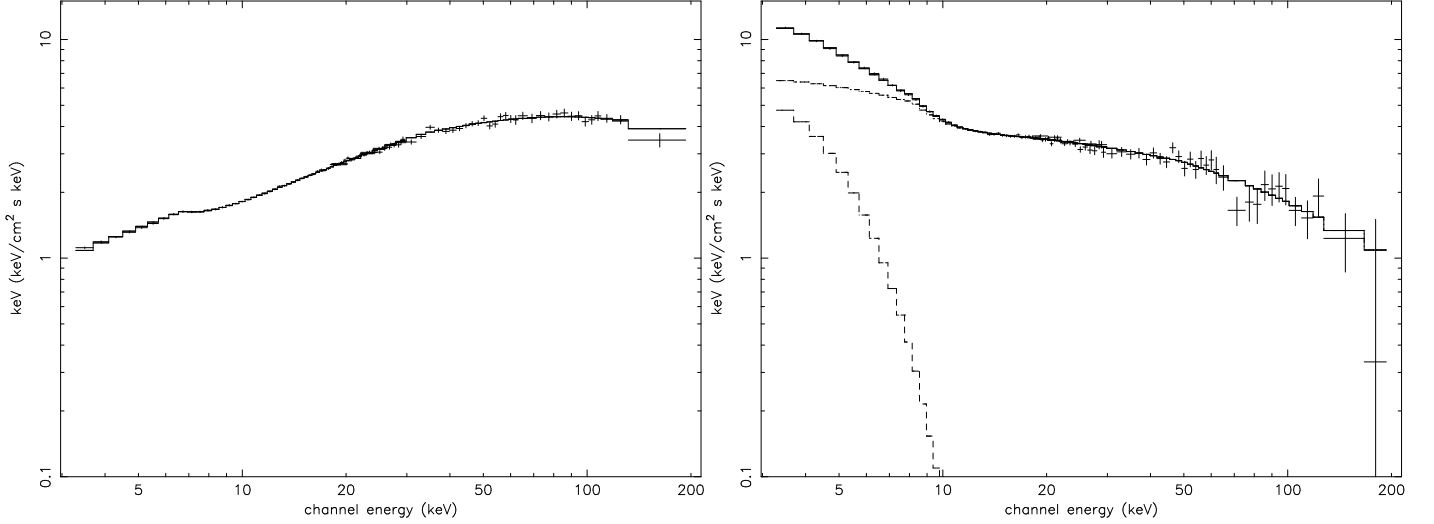


FIG. 1.— PCA (3 – 30 keV) and HEXTE (18 – 200 keV) unfolded spectra. *Left* shows a typical LS spectrum, with the best fit model (see the text for the details of the modeling) over-plotted (line). *Right* is a IS spectrum showing the different spectral components (dashed) used in the fits, *i.e.* a multicolor disk black body plus a power law. The best fit model is over-plotted as a line. The spectra are in “ $\nu F_\nu$ ” units.

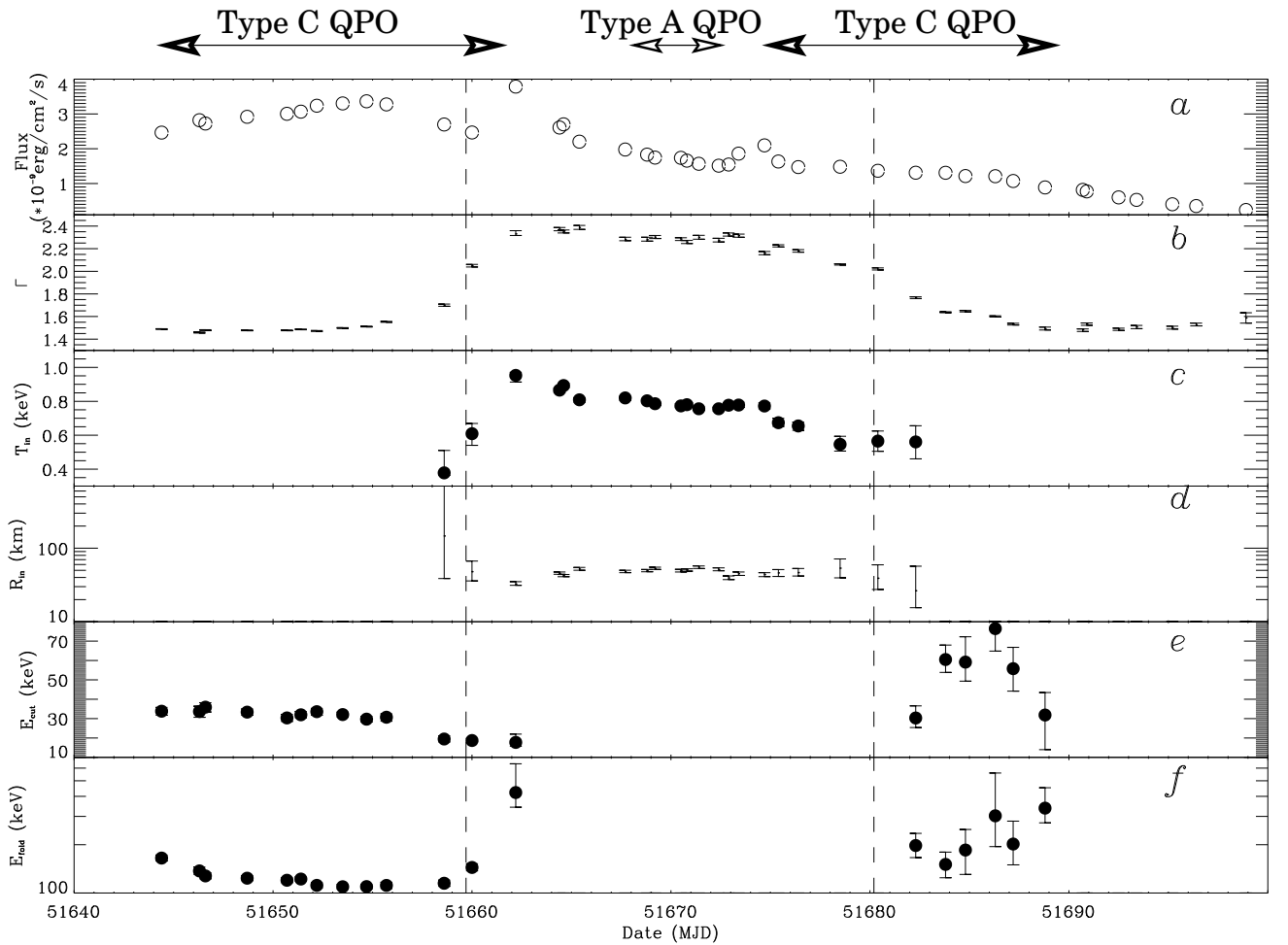


FIG. 2.— Evolution of the spectral parameters over the outburst. *a*) 2–200 keV light curve of the outburst. *b*) Power law spectral index  $\Gamma$ . *c*) Inner disk temperature (keV). *d*) Inner disk radius (assuming  $D=6$  kpc and  $i = 73.1^\circ$ ). *e*) cut-off energy (keV). *f*) e-folding of the cut-off (keV). The vertical dashed lines represent the dates of state transitions. The arrows on top of the plot show the dates where QPO are detected and to which type they belong (see paper 1).

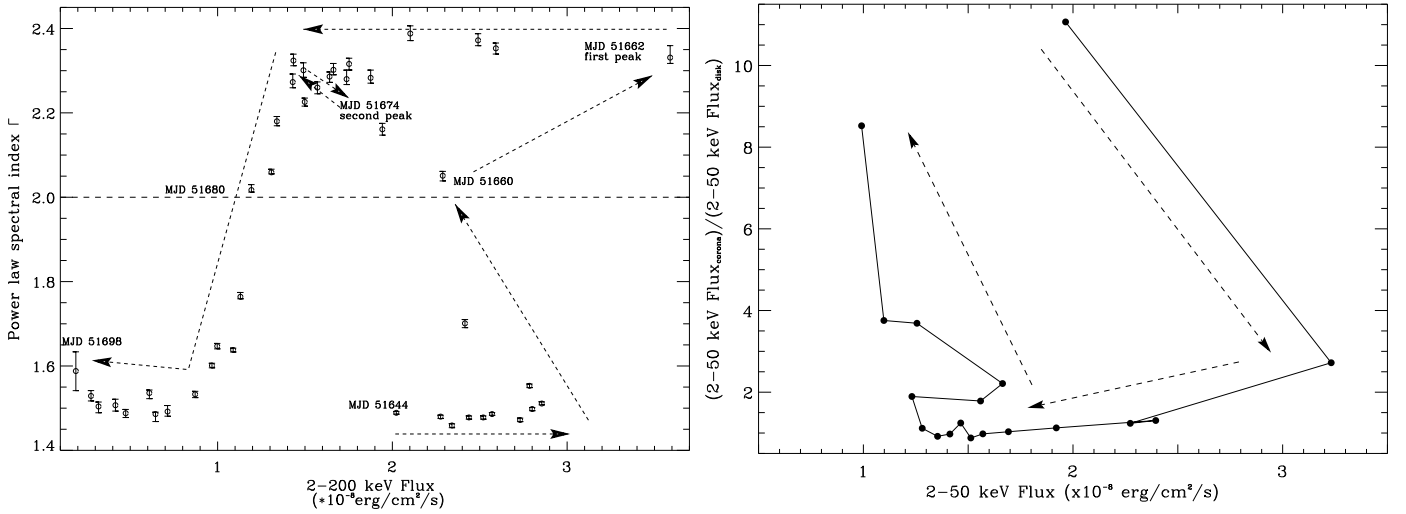


FIG. 3.— **Left** : Evolution of the power law photon index  $\Gamma$  vs. the 2–200 keV flux for the whole period of outburst. The hysteresis discussed in the text is clearly visible on this figure. The horizontal line separates the two states, and the arrows indicate the chronology of the events. Some dates, showing special events, have been reported. **Right** : Ratio of the fluxes of the powerlaw component (corona) to the multi-color disk component versus the source flux. The errors are left unplotted for the sake of clarity. This plot allows for a direct comparison with the neutron star system Aql X–1 (Maccarone & Coppi 2003). The arrows indicate the chronology of the outburst.

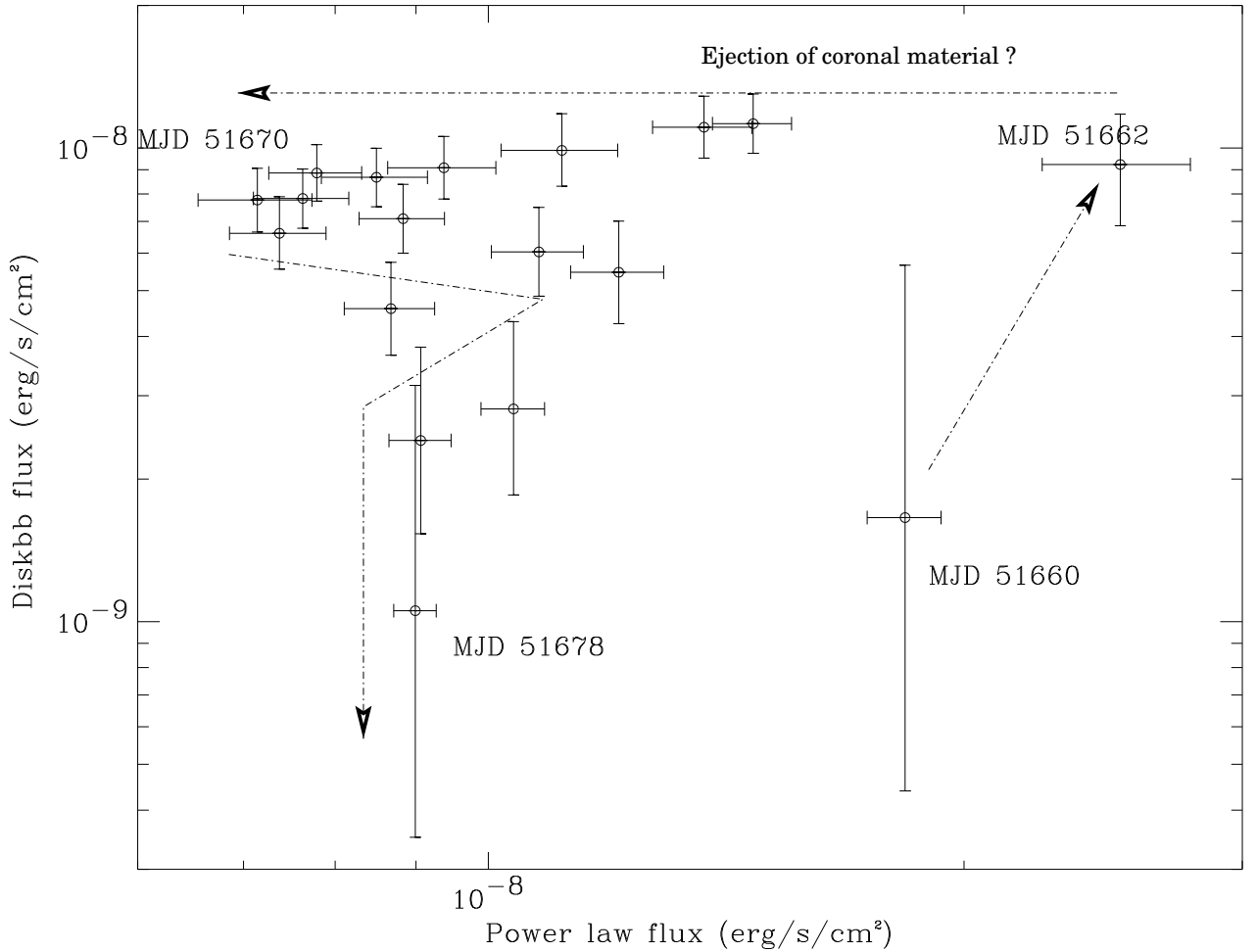


FIG. 4.— Evolution of the disk blackbody 2–50 keV flux vs. the power-law 2–50 keV flux. The arrows indicate the chronology of the events starting at the first transition on MJD 51660, and lasting on MJD 51678. Due to high uncertainties on the disk parameters, the points corresponding to MJD 51658, 51680 and 51682 are not represented here for the sake of clarity.